Study of the Reactions $^{16}O(^6Li, ^3He)^{19}F$ and $^{16}O(^6Li, t)^{19}Ne$ at $E(^6Li) = 24$ MeV*

J. D. Garrett,† H. G. Bingham, H. T. Fortune, and R. Middleton
Department of Physics, University of Pennsylvania, Philadelphia, Pennsylvania 19104
(Received 29 November 1971)

At a bombarding energy of 24 MeV, angular distributions have been measured for the reactions $^{16}O(^6Li, ^3He)^{19}F$ and $^{16}O(^6Li, t)^{19}Ne$. A distorted-wave Born-approximation (DWBA) analysis in the zero-range three-nucleon-cluster-transfer approximation has been performed. The sensitivity of the DWBA calculations on ^6Li parameters was demonstrated, with 160–190-MeV real-well-depth ^6Li parameters giving the best fits. By using Watson's ^6Li parameters, it was possible to account for the observed differences between the $(^6Li, ^3He)$ and $(^6Li, t)$ cross sections. The extracted relative spectroscopic strengths are consistent with the known structure of the final states.

I. INTRODUCTION

In recent years, several lithium-induced three-nucleon-transfer reactions have been studied[1-5] on light targets. Most recently, a predominantly direct-reaction mechanism has been suggested[1] for the strong transitions observed in the reactions $^{16}O(^6Li, ^3He)^{19}F$ and $^{16}O(^6Li, t)^{19}Ne$ at a bombarding energy of 24 MeV. It has also been suggested[6-8] that strong $(^3He, ^6Li)$ transitions proceed by the direct pickup of a three-nucleon cluster. The strength of these transitions reflects the structure of the final states and the magnitude[9,10] of the ^3He-t clustering in the ^6Li ground state – which is comparable[9,10] to the magnitude of the α-d clustering.

If the ^6Li-induced three-nucleon-transfer reactions proceed by a direct mechanism, then the extraction of quantitative spectroscopic information from the experimental data becomes possible. Such reactions then offer the possibility of studying the detailed spectroscopy of complex multiparticle, multihole states. However, the extraction of exact spectroscopic information is still difficult because of the problems involved in calculating realistic multinucleon form factors. In order to extract meaningful information it is necessary to make assumptions about the internal structure of the transferred three-nucleon system. For example, the effects of coherence are well documented[11] for two-nucleon transfer. Such effects may be even more important when three nucleons are transferred.

In the present study, additional evidence supporting the predominance of a direct mechanism for the ^6Li-induced three-nucleon-transfer reactions is presented in the form of angular distributions for the reactions $^{16}O(^6Li, ^3He)^{19}F$ and $^{16}O(^6Li, t)^{19}Ne$. In spite of the difficulties previously discussed, we have attempted a distorted-wave Born-approximation (DWBA) analysis of the stronger transitions, using simple assumptions. While such an approach is not justifiable, *a priori*, the reasonable agreement between the predictions and the data for the strong transitions provides the justification *a posteriori*.

II. EXPERIMENTAL PROCEDURE AND RESULTS

Angular distributions of the reactions $^{16}O(^6Li, ^3He)$-^{19}F and $^{16}O(^6Li, t)^{19}Ne$ were measured in $7\frac{1}{2}°$ intervals from $7\frac{1}{2}$ to $82\frac{1}{2}°$ (lab) by making a single exposure in the University of Pennsylvania multiangle spectrograph for each reaction. The bombarding energy was 24.0 MeV. The reaction products were identified by selectively scanning Ilford K2 and K-1 nuclear emulsions for triton and helium-3 tracks, respectively. 2- and 5-mil Mylar absorbers were placed in front of the emulsions for the $^{16}O(^6Li, ^3He)$ and $^{16}O(^6Li, t)$ reactions, respectively, to absorb the scattered ^6Li ions and other heavier reaction products. Because of the large energy loss of Li ions in matter, it was necessary to use a gas target assembly having no entrance window.[12] The gas target allowed the calculation of the absolute cross sections to an accuracy of ±15% and made possible a detailed comparison of the $^{16}O(^6Li, ^3He)$ and $^{16}O(^6Li, t)$ transition strengths. The use of "thin" gas targets, 20 Torr (34 $\mu g/cm^2$) and 16 Torr (27 $\mu g/cm^2$) for the $(^6Li, ^3He)$ and $(^6Li, t)$ reactions, respectively, made possible a resolution of about 35 keV full width at half maximum.

Energy spectra of the two reactions obtained at a lab angle of $7\frac{1}{2}°$ are presented in Fig. 1. These reactions are observed to selectively populate the members of the ground-state ($K^\pi = \frac{1}{2}^+$) rotational band, and to a lesser extent, the members of the four-particle–one hole ($K^\pi = \frac{1}{2}^-$) rotational band. The members of these bands are summarized in

Table I. For example, the $\frac{3}{2}^+$ member of the ground-state band is populated more than 20 times as strongly as the second $\frac{3}{2}^+$ state (at 3.92 and 4.04 MeV in ^{19}F and ^{19}Ne, respectively). As previously suggested,[1] such selectivity is evidence for a predominantly direct-reaction mechanism for the strong transitions and makes possible the mirror identification[1] of states in the nuclei ^{19}F and ^{19}Ne. The population of the high-spin states (e.g., the $\frac{7}{2}^+$ and $\frac{9}{2}^+$ states) – which could not be reached via single-nucleon transfer – indicates that these reactions could provide an excellent means of searching for high-spin states of simple configurations, e.g., $(j_n)^2 j_p$ coupled to large J.

Angular distributions of the ^{16}O(^{6}Li, ^{3}He) (points) and ^{16}O(^{6}Li, t) (crosses) reactions to members of the known (see Ref. 1 and references therein) $K^\pi = \frac{1}{2}^+$ and $\frac{1}{2}^-$ rotational bands are shown in Figs. 2 and 3. These angular distributions are observed to be forward-peaked, and similar in nature to the angular distributions of other Li-induced reactions[2,11-14] that have been interpreted as proceeding by a direct mechanism. The ^{16}O(^{6}Li, ^{3}He) angular distribution to the ground state of ^{19}F is very similar to the angular distribution of the time-reversed ^{19}F(^{3}He, ^{6}Li) transition[7] to the ground state of ^{16}O. The center-of-mass energy for the outgoing ^{6}Li in that study was 13.59 MeV to be compared with 17.45-MeV c.m. incident ^{6}Li in the present study. The general shapes of the other (^{6}Li, ^{3}He) and (^{6}Li, t) angular distributions are similar to those observed for ^{19}F(^{3}He, ^{6}Li) transitions[8] to the excited states of ^{16}O.

Three interesting features are observed in the comparison of the (^{6}Li, ^{3}He) and (^{6}Li, t) angular distributions: (1) The shapes of the angular distributions to mirror states in ^{19}F and ^{19}Ne are very similar; (2) both the (^{6}Li, ^{3}He) and (^{6}Li, t) cross sections are observed to increase with increasing spin up to the spin-$\frac{9}{2}$ states, and then to decrease for higher spins and higher excitation energies; (3) the strengths of the (^{6}Li, ^{3}He) and (^{6}Li, t) transitions to mirror states are comparable for the low-lying states; however, with increasing excitation energy, the (^{6}Li, t) transitions become weaker than the corresponding (^{6}Li, ^{3}He) transitions.

Hopefully, it should be possible to explain these three features in terms of simple DWBA calculations. Assuming isospin invariance of the nuclear force and ignoring the effects of the Coulomb force, these two reactions should be the same. Thus the similarity of the shapes and magnitudes (for the low-lying states) of the (^{6}Li, ^{3}He) and (^{6}Li, t) angular distributions is qualitatively understood. However, we shall see below that in order to explain the observed differences in the strength of the (^{6}Li, ^{3}He) and (^{6}Li, t) transitions (e.g., to the $\frac{9}{2}^+$ member of the ground-state band), it is necessary to include the effects of Coulomb distortion in the

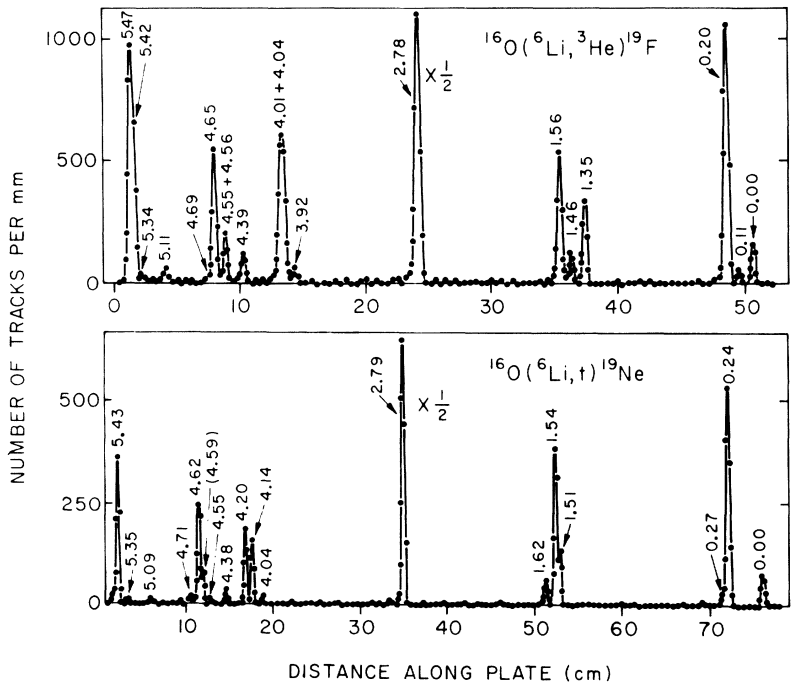

FIG. 1. Spectra of the reactions ^{16}O(^{6}Li, ^{3}He)^{19}F (top) and ^{16}O(^{6}Li, t)^{19}Ne (bottom) obtained at a bombarding energy of 24 MeV and a laboratory angle of 7.5°. Energies are in MeV.

exit channels and the differences in the reaction Q values for transitions to the mirror states. [The ground-state Q values are -4.094 and -7.350 MeV for the (^{6}Li, ^{3}He) and (^{6}Li, t) reactions, respectively.] The analysis of the angular distributions in the DWBA formalism is discussed in the following section.

III. DWBA ANALYSIS

Based on the evidence that the ^{6}Li-induced three-nucleon stripping reaction is predominantly direct,[1] an attempt has been made to describe the (^{6}Li, ^{3}He) and (^{6}Li, t) transitions to the low-lying members of the ground-state band using the DWBA formalism. Even though the inadequacies of such an analysis are well known, it was hoped that some of the interesting features observed in the angular distributions could be reproduced by the calculations. The success or failure of such a procedure may suggest possible improvements or alternatives.

DWBA cross sections were calculated in the zero-range approximation with local potentials using the code DWUCK.[15] In the ^{3}He-t cluster description of the ^{6}Li ground state, the ^{3}He and triton exist in a relative s state in which the ^{3}He-t wave function is suggested[10] to be appreciably more localized than the α-d wave function. Thus the zero-range assumption may have some validity. Indeed, in the (d, ^{6}Li)[16] and (^{6}Li, d)[17] reactions, the results of finite-range calculations have been observed to differ only slightly from those of zero-range calculations.

TABLE I. Known rotational bands in ^{19}F and ^{19}Ne.

K^π	J^π	Excitation energy [a] ^{19}F	^{19}Ne
$\frac{1}{2}^+$	$\frac{1}{2}^+$	0.00	0.00
	$\frac{3}{2}^+$	1.56	1.54
	$\frac{5}{2}^+$	0.20	0.24
	$\frac{7}{2}^+$	5.47	5.43
	$\frac{9}{2}^+$	2.78	2.79
	$\frac{11}{2}^+$	(6.50) [b]	c
	$\frac{13}{2}^+$	4.65	4.62
$\frac{1}{2}^-$	$\frac{1}{2}^-$	0.11	0.27
	$\frac{3}{2}^-$	1.46	1.62
	$\frac{5}{2}^-$	1.35	1.51
	$\frac{7}{2}^-$	4.01	4.14 [d]
	$\frac{9}{2}^-$	4.04	4.20 [d]

[a] Band member assignments are from the literature as summarized in Ref. 1.

[b] This is the only known low-lying $\frac{11}{2}^+$ state in ^{19}F [see J. H. Aitken, K. W. Allen, R. E. Azuma, A. E. Litherland, and D. W. O. Rogers, Phys. Letters 28B, 653 (1969)]. This level, however, was not strongly populated in the ^{16}O(^{16}Li, ^{3}He) reaction, whereas other known members of this band were.

[c] Not known.

[d] These two levels may possibly be reversed in ^{19}Ne, i.e., the 4.14 being the $\frac{9}{2}^-$ band member and the 4.20 being the $\frac{7}{2}^-$ member.

The bound-state form factor was calculated in the "three-nucleon-transfer approximation[16]"; i.e., the internal structure of the three-nucleon cluster in the final state was assumed to be the same as it is in ^{6}Li. The cluster wave function was taken to be an eigenfunction of the Hamiltonian describing the motion of a particle of mass 3 and spin $\frac{1}{2}$ in a real Woods-Saxon-plus-Coulomb potential. Bound-state geometrical parameters $r_0 = r_{0c} = 2.0$ F and $a = 0.65$ F were used in all the calculations. These are the values that were used in the DWBA analysis of a recent ^{19}F(^{3}He, ^{6}Li)^{16}O study[7] and are of a similar magnitude to those used in analysis of (d, ^{6}Li) reactions on light nuclei.[16] The rather large value for r_0 and r_{0c} reflects the finite size of the bound three-nucleon cluster. No spin-orbit force was included in the bound-state calculations. For the ground-state band, it was assumed that the three nucleons were added to the sd shell [i.e., $2(N-1)+L=6$].

All calculations discussed herein used the same optical-model parameters in the exit channel (Table II). [The use of the same optical-model parameters for the ^{3}He and t exit channels is justified, since the isospin-dependent term of the optical-model potential ($\propto \vec{t}\cdot\vec{T}_f$) has the same value for the ^{3}He + ^{19}F channel as for the t + ^{19}Ne channel.] These parameters are those used in an analysis of the reaction ^{19}F(^{3}He, ^{6}Li)^{16}O and are of the same discrete family as the ^{3}He parameters used in analysis of one- and two-nucleon-transfer reactions in this mass region.[11] Calculations using other mass-3 parameters were performed with no significant improvement in the fits.

One of the difficulties encountered in the DWBA analysis of Li-induced reactions has been the lack of good optical-model parameters for Li scattering. Recently, several new sets of ^{6}Li parameters have appeared in the literature. In the present analysis, we have used six separate sets of ^{6}Li parameters, all of which are listed in Table II.

Parameter Set 1 has been used in an analysis of the time-reversed reaction[7] ^{19}F(^{3}He, ^{6}Li)^{16}O(g.s.). This set also gave a good fit to the elastic scattering data.[7,18,19] Parameter Sets 2 and 3 are due to Watson,[20] who fitted elastic ^{16}O + ^{6}Li data of Bethge, Fou, and Zurmühle.[21] Watson's real well depth ($V = 159$ MeV for ^{6}Li + ^{16}O) is shallower than 6

TABLE II. Optical-model parameters used in DWBA calculations of the reactions $^{16}O(^6Li, ^3He)^{19}F$ and $^{16}O(^6Li, t)^{19}Ne$.

Channel	V_0 (MeV)	W (MeV)	$W'=4W_D$ (MeV)	r_0 (F)	a (F)	r_C (F)	r'_0 (F)	a' (F)	Reference
^{6}Li									
Set 1	190.0	0	47.32	1.05	0.89	2.50	1.95	0.55	7
Set 2	159.0	0	34.0	1.24	0.78	2.50	1.55	0.80	20
Set 3	159.0	7.0	0	1.23	0.78	2.50	2.15	0.80	20
Set 4	37.8	0	32.28	1.42	0.95	2.50	1.90	0.62	21
Set 5	60.3	4.6	0	1.47	0.75	2.50	2.29	0.85	21
Set 6	171.0	7.24	0	1.33	0.67	2.50	1.45	0.72	22
^{3}He-t	155.2	18.8	0	1.15	0.73	1.40	1.55	0.70	7
Bound state	a	...	...	2.0	0.65	2.0	...	...	7

[a] The bound-state well depths were adjusted to give the $t/^3$He a binding energy of $B=-[15.79+Q(^6Li, ^3He-t)]$ MeV.

times the single-nucleon potential (~300 MeV) – as expected as a consequence of the Pauli principle. Sets 2 and 3 differ mainly in the radial form of the absorptive potential – Set 2 has surface-peaked absorption; whereas, Set 3 has volume absorption.

Parameter Sets 4 (surface absorption) and 5 (volume absorption) were derived from the original analysis[21] of the 20-MeV elastic $^6Li+^{16}O$ scattering. In that analysis, all parameters were allowed to vary in order to obtain a best fit for the elastic scattering of ^{6}Li on ^{16}O. Set 6 was obtained[22] by fitting 13-MeV $^6Li+^{12}C$ elastic-scattering data and has been used[22] in a DWBA analysis of the reaction $^{12}C(^6Li, \alpha)^{14}N$ at bombarding energies of 12 and 14 MeV.

Results of calculations using these parameters for the $^{16}O(^6Li, ^3He)^{19}F$(g.s.) transition are compared with the data in Fig. 4. The agreement for ^{6}Li parameter Set 1 is striking. The predictions of Sets 2 and 3 are in excellent agreement with

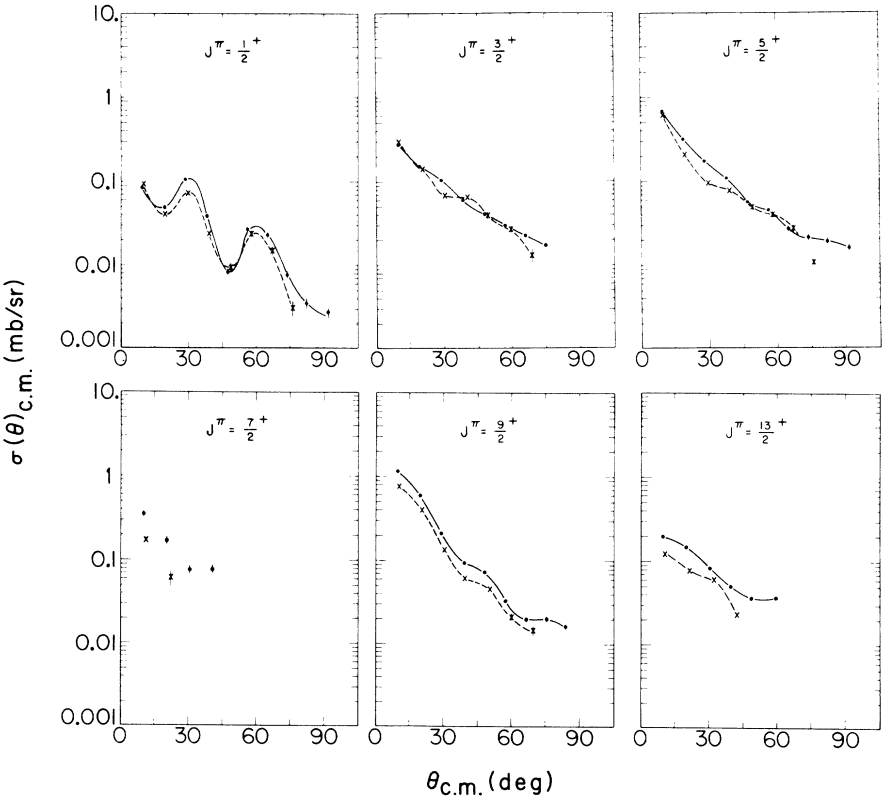

FIG. 2. Angular distributions for the $^{16}O(^6Li, ^3He)^{19}F$ (points) and $^{16}O(^6Li, t)^{19}Ne$ (crosses) reactions to mirror states in the ground-state rotational bands of ^{19}F and ^{19}Ne. The curves serve only as guides to the eye.

the data for the first two maxima, but they predict the third maximum at a larger angle (~10°) than observed. Set 6 predicts the position of the maxima correctly, but the magnitudes of successive maxima are not at all reproduced. Set 5 reproduces the second maximum, but the calculations and the data become grossly out of phase at larger angles. Set 4 does not even correctly predict the position of the second maximum.

It is perhaps not surprising that calculations based on parameter Set 1 agree well with the ^{16}O-(^{6}Li, ^{3}He)^{19}F ground-state transition. Calculations using this set in conjunction with the ^{3}He parameter set used in the present study give a good fit to the time-reversed reaction ^{19}F(^{3}He, ^{6}Li)^{16}O. It can be seen that the ^{6}Li parameter sets having a real-well depth of 159–190 MeV (Table II) are the most successful in reproducing the shape of the ground-state angular distribution. In an analysis of the ^{19}F(^{3}He, ^{6}Li)^{16}O ground-state transition, it was found[7] that reasonable fits were obtained only when the ^{3}He real-well potentials, $V_{^3\mathrm{He}}$, were used in combination with the next deeper ^{6}Li family, i.e., $V_{^6\mathrm{Li}} \approx V_{^3\mathrm{He}} + 40$ MeV. This same criterion also seems to have some significance in the present study. It might be expected that in three-nucleon stripping and pickup reactions the entrance- and exit-channel real potentials should differ by three single-nucleon potentials (i.e., ≈150 MeV). It is interesting, however, that the real well depth necessary to correctly bind the three-nucleon cluster is about 50 MeV.

The dependence of the DWBA angular distributions on the lower-cutoff (LCO) radius was used to investigate contributions of the nuclear interior. This dependence is demonstrated in Fig. 5 for the ^{16}O(^{6}Li, ^{3}He)^{19}F ground-state transition. It is observed that the cross section near the first two maxima remains relatively constant (i.e., within 30%) for LCO's inside the nuclear radius. The changes in shape and magnitude for cutoffs within the nucleus largely reflect the oscillations in the distorted waves. A cutoff just outside the nuclear surface (LCO = 6 F) gives a forward-angle cross section that does not differ drastically from that for LCO = 0. The angular distribution predicted for LCO = 6 F, however, falls off less rapidly with increasing angle than does the one for LCO = 0. The predictions based on LCO's outside the nuclear radius demonstrate that the main contri-

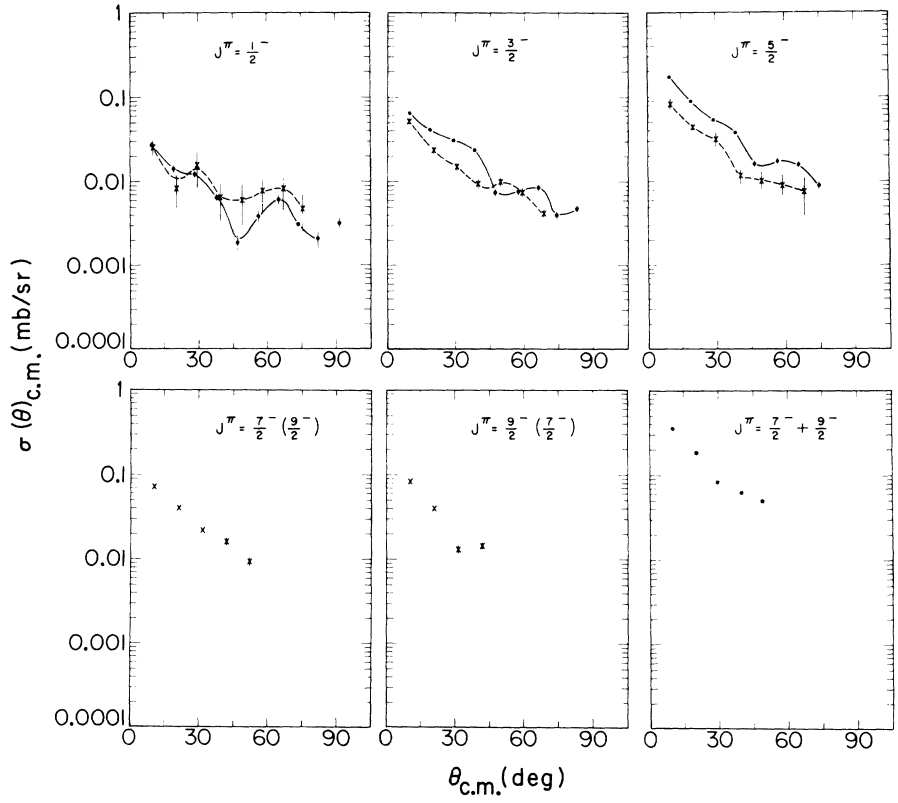

FIG. 3. Angular distributions for the reactions ^{16}O(^{3}Li, ^{3}He)^{19}F (points) and ^{16}O(^{6}Li, t)^{19}Ne (crosses) to mirror states in the $K^\pi = \frac{1}{2}^-$ rotational bands in ^{19}F and ^{19}Ne. The curves serve only as guides to the eye.

butions to the reaction cross section come from radii between 6 and 7 F. The fact that the interior contributes only slightly in the present case means that our simplified assumption for the form factor will not greatly affect the results, since the form factor does have the correct asymptotic behavior. The calculations discussed below were all obtained for LCO = 0.

Figure 6 compares the results of DWBA calculations with the experimental angular distributions of the $\frac{1}{2}^+$, $\frac{3}{2}^+$, $\frac{5}{2}^+$, and $\frac{9}{2}^+$ members of the ground-state rotational band for both the $^{16}O(^6Li, ^3He)$ and $^{16}O(^6Li, t)$ reactions. The solid and broken curves correspond to calculations using parameter Sets 1 and 3, respectively. As remarked earlier, the agreement for parameter Set 1 is excellent for transitions to the $\frac{1}{2}^+$ ground states. The $l=2$ distributions of the $\frac{3}{2}^+$ and $\frac{5}{2}^+$ states are not as well reproduced by the calculations; however, the general trend of the experimental data is reproduced. The experimental data for the $l=4$ transitions to the $\frac{9}{2}^+$ states fall off faster than predicted. The calculations with parameter Set 3 give somewhat better agreement than those using Set 1 for the $l=2$ and 4 experimental distributions. Calculations with parameter Set 2 were similar to those for Set 3.

The ratio of the experimental to calculated cross sections ($\sigma_{Exp}/\sigma_{DWUCK}$) obtained from the fits shown in Fig. 4 are presented in Table III. Values are tabulated for the three parameter sets (i.e., Sets 1, 2, and 3) which produced reasonable agreement with the experimental data. If the DWBA correctly accounts for effects of distortion and the reaction kinematics, the tabulated ($\sigma_{Exp}/\sigma_{DWUCK}$) ratios should be the same for mirror

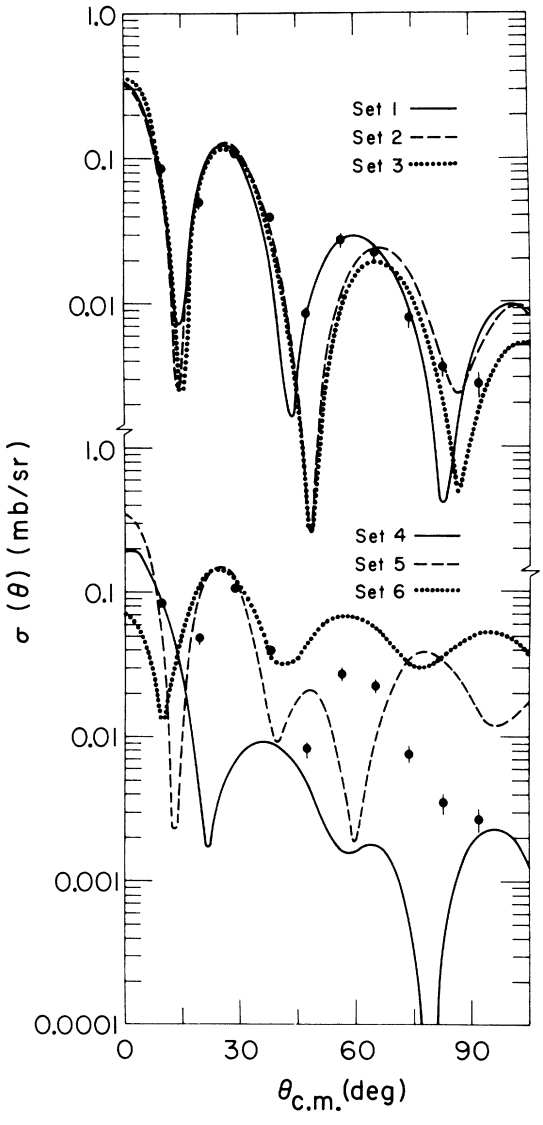

FIG. 4. Experimental angular distribution for the ^{16}O-$(^6Li, ^3He)^{19}F$(g.s.) transition (points) and results of DWBA calculations (curves) using the ^6Li potentials indicated. Parameters are listed in Table II.

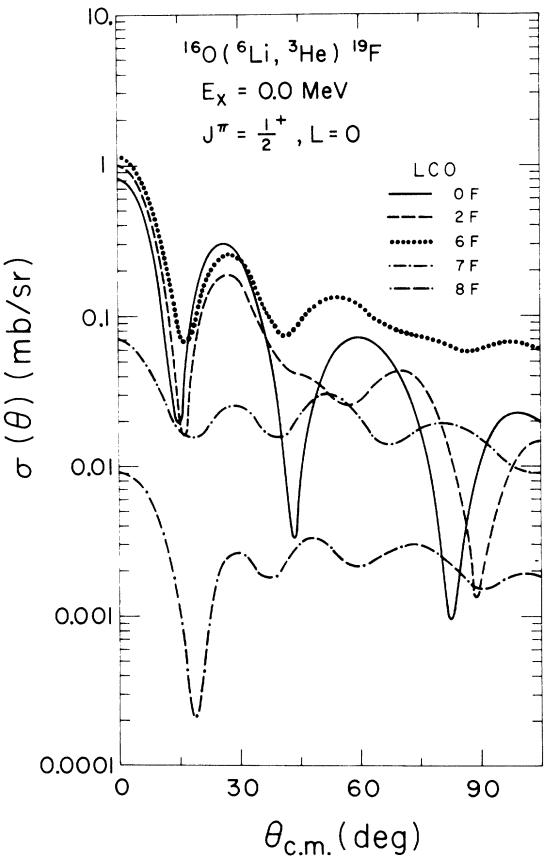

FIG. 5. Dependence of the DWBA calculations on the lower-cutoff radius (LCO). These calculations used ^6Li parameter Set 1.

TABLE III. Relative spectroscopic strengths.

	$^{16}O(^6Li, ^3He)^{19}F$				$^{16}O(^6Li, t)^{19}Ne$			
		$\sigma_{Exp}/\sigma_{DWUCK}$ [a]				$\sigma_{Exp}/\sigma_{DWUCK}$ [a]		
J^π	E_x (MeV)	Set 1 [b]	Set 2 [b]	Set 3 [b]	E_x (MeV)	Set 1 [b]	Set 2 [b]	Set 3 [b]
$\frac{1}{2}^+$	0.00	0.41	0.29	0.35	0.00	0.45	0.27	0.37
$\frac{3}{2}^+$	1.56	0.32	0.28	0.38	1.54	0.25	0.28	0.32
$\frac{5}{2}^+$	0.20	0.33	0.25	0.33	0.24	0.34	0.27	0.36
$\frac{9}{2}^+$	2.78	0.35	0.26	0.32	2.79	0.20	0.23	0.33
$\frac{7}{2}^+$ [c]	5.47	...	...	0.27	5.43	...	...	0.25

[a] See text for description of DWBA calculation.

[b] See Table II and text for description of parameters used. The same ^{3}He-t parameter set was used in all the calculations.

[c] Even though full angular distributions were not measured for the $\frac{7}{2}^+$ state, the DWBA calculations did correctly account for the difference in cross sections in the two reactions (see text).

states in ^{19}F and ^{19}Ne. For ^{6}Li parameter Sets 2 and 3, the ratios are observed to differ by <15% (<10% in all except two cases), even though the cross sections for the $\frac{9}{2}^+$ states differ by over 50%. The calculations using ^{6}Li parameter Set 1, however, do not properly reproduce the differences in cross sections observed in the two reactions.

Since the intrinsic state corresponding to the ground-state band of ^{19}F and ^{19}Ne is nearly identical to the cluster-model state,[23] all members of this band should be populated with comparable spectroscopic strengths.[14,24] This is indeed the case. The ratios $\sigma_{Exp}/\sigma_{DWUCK}$, extracted using parameter Sets 2 and 3, differ by <20% for the members of this band.

Complete angular distributions for the $\frac{7}{2}^+$ members of the ground-state band were not measured (see Fig. 2), because of the difficulty of detecting low-energy exciting particles. Because of insufficient experimental data for the $\frac{7}{2}^+$ states and the poorer fit for the $l=4$ transfer at forward angles (Fig. 6) no distorted-wave calculations are shown for the $\frac{7}{2}^+$ states. However, DWBA calculations based on ^{6}Li parameter Sets 2 and 3 do predict the observed difference (Fig. 2) in (^{6}Li, ^{3}He) and (^{6}Li, t) cross sections for the $\frac{7}{2}^+$ members of this rotational band.

A distorted-wave analysis was also attempted for angular distributions of the states belonging to the $K^\pi = \frac{1}{2}^-$ rotational band (see Fig. 3). The agreement between the predicted and measured angular distributions, however, was poorer than for the positive-parity band. Perhaps the most interesting feature of the angular distributions for the negative-parity states is the similarity between the $\frac{1}{2}^+$ and $\frac{1}{2}^-$ angular distributions, and between those for $\frac{3}{2}^+$ and $\frac{3}{2}^-$ and those for $\frac{5}{2}^+$ and $\frac{5}{2}^-$. One would perhaps have expected the $\frac{1}{2}^-$ and $\frac{3}{2}^-$ angular distributions to be similar to each other and to be described by an $l=1$ DWBA calculation. Such is not the case. The $\frac{1}{2}^-$ angular distributions are much more similar to the $\frac{1}{2}^+$ angular distributions that to those for the $\frac{3}{2}^-$ states. These characteristics of the negative-parity states are not at all reproduced by the DWBA calculations. Two factors

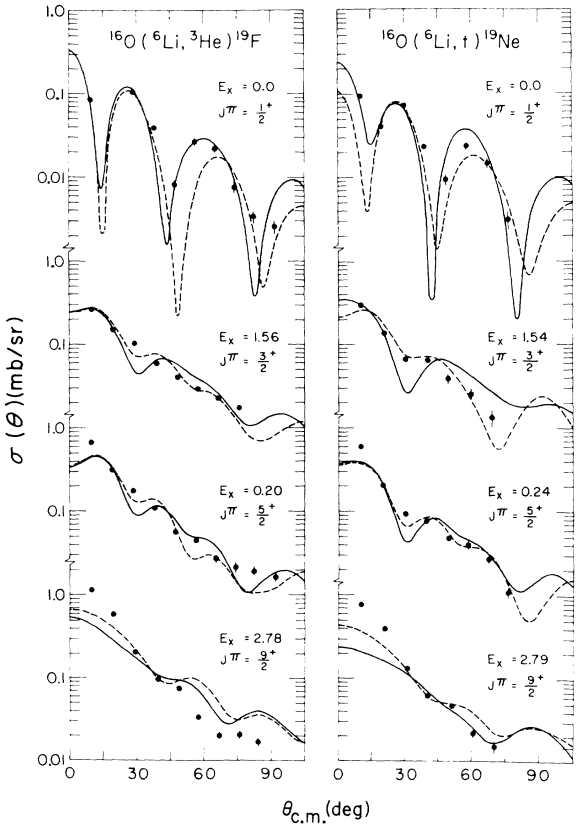

FIG. 6. Experimental (points) and theoretical (curves) angular distributions for the reactions $^{16}O(^6Li, ^3He)^{19}F$ and $^{16}O(^6Li, t)^{19}Ne$ populating mirror states in the ground-state rotational bands of ^{19}F and ^{19}Ne. The solid curves were obtained using ^{6}Li parameter Set 1, the dashed curves Set 3.

which may contribute to the poorer agreement for the negative-parity band are: (1) The negative-parity band is more weakly excited; hence, contributions from reaction mechanisms other than direct three-nucleon transfer may be more important. This possibility is consistent with the fact that these states were more weakly populated relative to the members of the $K^\pi = \frac{1}{2}^+$ band in a recent $^{16}O(^6Li, t)^{19}Ne$ study[4] at an incident energy of 36 MeV than they were in the present study at 24 MeV. (2) The members of the negative-parity band, which are believed to be based predominantly on a $1p$-shell hole[12,23] may be populated by the transfer of more than one configuration. They may, e.g., be excited through either the two-particle–two-hole or four-particle–four-hole components in the ^{16}O ground state, as well as by adding one of the nucleons to the $1f$-$2p$ shell. (For deformed nuclei one of the single-particle orbitals from the $1f$-$2p$ shell is expected to come quite low in excitation for large deformation.[11]) Therefore, the effects of coherence may be more important in the transitions to the negative-parity band than for the positive-parity band, where the predominant configuration is three $2s$-$1d$-shell nucleons outside a closed ^{16}O core.[23]

IV. CONCLUSIONS

A zero-range DWBA analysis based on the transfer of a three-nucleon cluster is successful in reproducing the angular-distribution shapes and the relative strengths of the members of the $K^\pi = \frac{1}{2}^+$ ground-state rotational bands in ^{19}F and ^{19}Ne populated by the $^{16}O(^6Li, ^3He)$ and $^{16}O(^6Li, t)$ reactions. This success supports the suggestion[1] that these states are populated by a predominantly direct-reaction mechanism at 24-MeV incident energy. The sensitivity of the DWBA calculations to ^6Li parameters was demonstrated, with the 160–190-MeV real-well-depth ^6Li parameters giving the best fits. By using the Watson ^6Li parameters,[20] it was possible to account for the observed differences between the $(^6Li, ^3He)$ and $(^6Li, t)$ cross sections. The extracted relative transition strengths are consistent with the known structure of the final states within the $K^\pi = \frac{1}{2}^+$ g.s. band. The over-all agreement resulting from the simple zero-range, three nucleon-cluster-transfer approximation is probably better than one would have expected *a priori*, and gives encouragement for future DWBA calculations for ^6Li-induced transfer reactions.

ACKNOWLEDGMENTS

The authors thank J. W. Watson for furnishing us his ^6Li optical-model parameters prior to their publication. We also acknowledge interesting discussions with R. M. Drisko, O. Hansen, C. H. Holbrow, and U. Strohbusch. We are grateful to J. Cizewski for her assistance in the data analysis, and to M. Barnett and V. Adams for their meticulous scanning of the nuclear-emulsion plates.

---

*Supported by the National Science Foundation.

† Present address: Los Alamos Scientific Laboratory, University of California, Los Alamos, New Mexico 87544.

[1]H. G. Bingham, H. T. Fortune, J. D. Garrett, and R. Middleton, Phys. Rev. Letters 26, 1448 (1971).

[2]A. A. Oglobin, in *Proceedings of the International Conference on Nuclear Reactions Induced by Heavy Ions, Heidelberg, Germany, 15–18 July 1969,* edited by R. Bock and W. R. Hering (North-Holland, Amsterdam, 1970), p. 231.

[3]G. Bassani, T. H. Kruse, N. Saunier, and G. Souchere, Phys. Letters 30B, 621 (1969).

[4]H. E. Gove and A. D. Panagiotou, Bull. Am. Phys. Soc. 16, 490 (1971); and private communication.

[5]J. D. Garrett, H. G. Bingham, H. T. Fortune, and R. Middleton, Bull. Am. Phys. Soc. 16, 511, 1148 (1971).

[6]F. C. Young, P. D. Forsyth, M. L. Roush, W. F. Hornyak, and J. B. Marion, Phys. Letters 13, 50 (1964); R. O. Mead and F. C. Young, Nucl. Phys. A115, 161 (1968); W. J. Klages, H. H. Duhm, H. Yoshida, P. E. Schumacher, and C. Detraz, *ibid.* A156, 65 (1970).

[7]U. Strohbusch, W. Schmidt, and G. Huber, Nucl. Phys. A163, 453 (1971).

[8]C. Detraz, C. E. Moss, C. D. Zafiratos, and C. S. Zaidins, Nucl. Phys. A167, 337 (1971).

[9]A. M. Young, S. L. Blatt, and R. G. Seyler, Phys. Rev. Letters 25, 1764 (1970); and R. D. Amado and J. V. Noble, Phys. Rev. C 3, 2494 (1971), and references therein.

[10]I. V. Jurdyumov, V. G. Neudatchin, and Y. F. Smirnov, Phys. Letters 31B, 426 (1970).

[11]J. D. Garrett, R. Middleton, D. J. Pullen, S. A. Andersen, O. Nathan, and O. Hansen, Nucl. Phys. A164, 449 (1971), and references therein.

[12]R. Middleton, in *Proceedings of the International Conference on Nuclear Reactions Induced by Heavy Ions, Heidelberg, Germany, 15–18 July 1969,* edited by R. Bock and W. R. Hering (North-Holland, Amsterdam, 1970) p. 263.

[13]K. Bethge, Ann. Rev. Nucl. Sci. 20, 255 (1970).

[14]P. Neogy, W. Scholz, J. Garrett, and R. Middleton, Phys. Rev. C 2, 2149 (1970).

[15]P. D. Kunz, University of Colorado Report No. COO-535-613 (unpublished).

[16]L. J. Denes, W. W. Daehnick, and R. M. Drisko, Phys. Rev. 148, 1097 (1966).

[17]K. Kubo and M. Hirata, to be published.

[18]G. Scheklinski, U. Strohbusch, and B. Goel, Nucl. Phys. A153, 97 (1970).

[19]W. Schmidt and U. Strohbusch, Nucl. Phys. A159, 104 (1970).
[20]J. W. Watson, private communication.
[21]K. Bethge, C. M. Fou, and R. W. Zurmühle, Nucl. Phys. A123, 521 (1969).
[22]D. J. Johnson and M. A. Waggoner, Phys. Rev. C 2, 41 (1970).
[23]H. G. Benson and B. H. Flowers, Nucl. Phys. A126, 305 (1969).
[24]V. V. Davidow and L. M. Pavlichenkov, Phys. Letters 29B, 551 (1969).

PHYSICAL REVIEW C VOLUME 5, NUMBER 3 MARCH 1972

Pionic X-Ray Yields and $2p$-Level Widths in ^{6}Li, ^{9}Be, ^{12}C, and ^{16}O†

W. W. Sapp, Jr.,* M. Eckhause, G. H. Miller,‡ and R. E. Welsh
College of William and Mary, Williamsburg, Virginia 23185

(Received 7 September 1971)

We have measured the intensities of $2p$-$1s$ pionic x-ray transitions in ^{6}Li, ^{9}Be, ^{12}C, and ^{16}O using an absolute-efficiency technique. A pion-cascade calculation which was constrained to reproduce the observed yields predicted population probabilities for the mesonic levels and gave values for the strong-interaction level widths. The $2p$-level broadenings are 0.015 ± 0.005 eV for ^{6}Li, 0.16 ± 0.03 eV for ^{9}Be, 2.1 ± 0.6 eV for ^{12}C, and 12 ± 4 eV for ^{16}O. Comparisons are made with results obtained by others and with predictions based upon a semiphenomenological optical potential. Empirical capture schedules for π^- in ^{6}Li and ^{12}C are also presented.

I. INTRODUCTION

The yield, or intensity, of the $2p$-$1s$ pionic atomic transition, defined as the number of $K\alpha$ x rays emitted per stopped pion, can be used to deduce the nuclear-absorption rate for a pion in the $2p$ state.[1] Ericson and Ericson[2] have described the absorptive interaction in terms of an imaginary part of a semiphenomenological optical potential. A recent analysis by Krell and Ericson[3] has suggested that either this optical potential does not satisfactorily describe $2p$-state absorption for all elements or that a systematic uncertainty exists in one or both of the experimental methods used to determine the absorption rates. In particular, measurements in elements with $Z \leq 11$ were in substantial disagreement with predictions based on measurements in higher-Z elements. We wish to report here the first measurement of the $2p$-$1s$ pionic transition yield in ^{6}Li in addition to new measurements for ^{9}Be, ^{12}C, and ^{16}O. The yield in ^{9}Be is in excellent agreement with a recently reported value[4] from CERN, but is in disagreement with another measurement by Berezin *et al.*[5] Previously published[4,6] yields in ^{12}C and ^{16}O (as H_2O) which were based on comparisons between muonic and pionic x-ray spectra are substantially larger than those obtained in this investigation.

The results of the present work compare favorably with predictions based on an optical potential whose constant parameters have been independently determined[7] from selected pionic x-ray data. A secondary purpose of this investigation was to determine the capture schedule for π^- in ^{6}Li, for which no previous measurements exist. This capture schedule is of particular interest to those engaged in a theoretical comparison of radiative pion capture and muon capture in this element.[8] The capture schedule for ^{12}C is also presented because of apparent disagreements in the literature[9,10] on the interpretation of existing yield data.

II. EXPERIMENTAL TECHNIQUE AND DATA ANALYSIS

The data were obtained in two experiments using a 190-MeV/c negative-pion beam of the NASA Space Radiation Effects Laboratory (SREL) synchrocyclotron. Standard scintillation-counter coincidence techniques were used to obtain a π-stop signal. A 1600-channel analyzer sorted and stored pulses from a Si(Li) or Ge(Li) detector when a coincidence existed between the π-stop signal and the detector signal. The timing window for this coincidence was 320 nsec wide and was typically about 3 times the full width at 0.1 maximum of the timing peak. Other features of the experiment were the following:

(1) Absolute muonic x-ray yields were also measured to investigate systematic errors which might have arisen either in the experiments or in the data analysis. The muonic K series is particularly use-